Optimal Placement of Energy Storage in Distribution Networks

Yujie Tang and Steven H. Low

***Abstract*— We study the problem of optimally placing energy storage devices in distribution networks to minimize total energy loss, focusing on structural results. We use a continuous linearized branch-flow model to model the distribution network. For the special case of a linear network, modeling a main feeder, we explicitly derive the optimal solution when all loads have the same shape and prove several useful monotonicity properties of the optimal solution. We illustrate through simulations that these structural properties hold approximately also on radial networks modeled by standard discrete nonlinear power flow models and even when loads have different shapes. We discuss how these structural results provide insight for the planning of energy storage devices.**

I. Introduction

Energy storage devices shift energy generation and consumption across time and can help integrate volatile or intermittent generations and loads. There is a large literature motivated by the value and technological advances of storage technologies, e.g., [1], [2], [3], [4]. Research in the area of storage planning and operations can be roughly categorized into two types. One type assumes that the storage devices are used to maximize profit in the electricity market. For example, [5], [6] study the optimal operation and the value of storage owned by a single consumer, and [7] considers situations with renewable generations. The other type assumes that the storage devices are operated by system operators, and their objective is to minimize operational cost of the power system as well as to maintain grid reliability. For example, [8], [9], [10] propose algorithms for finding optimal placement of storage in grids; [11] proves some structural properties of optimal storage placement using the DC power flow model; [12] treats the stochastic control of distributed storage devices using a surrogate LQ problem, and [13] proposes a suboptimal algorithm for the stochastic control of distributed storage with performance guarantee. [14], [15], [16] propose methods to incorporate distributed energy storage systems with renewable generations, and conducts case studies to evaluate the benefit of storage. In [17], the authors study the locational marginal value of energy storage in a network when the energy capacity is small.

This paper belongs to the second category, where the operator of a distribution network has a total budget for energy storage and needs to decide where to deploy storage devices and their capacities so as to optimize the grid operation (in our case, minimize active power loss on the network). Since the operational cost depends both on the placement and sizing of storage devices as well as on their charging/discharging schedules, the time and space dimensions are strongly coupled. As many placement algorithms have already been proposed in the literature, we will instead focus on structural properties of the optimal solution that can provide insight for deployment. We use a simplified model but verify our results using standard and more realistic power flow models.

Our contribution is two-fold. First we propose a continuous linearized branch-flow model, based on the DistFlow model of [18], [19] for distribution systems. Linearized DistFlow model was first proposed in [18], [19] and used in the [20] for optimal power flow problems. The linearized model is accurate when the line loss is small compared with the branch power flow. It is more useful for distribution systems than the DC power flow model because it can be solved explicitly given the injections and a linear solution bounds a nonlinear solution; see [21, Section VI]. A continuous nonlinear DistFlow model has been used in [22] for analyzing long distribution feeder. We combine both ideas to obtain a simple model for analysis.

Second we derive several structural properties of optimal storage placement and sizing for a single line modeling a main feeder, when all loads have the same shape. For instance, there exists a special location ξ^* such that an optimal strategy will deploy no storage on any location between the substation and ξ^* and deploy storage on all locations beyond ξ^*. Moreover the scaled capacities increase along the line from ξ^* towards the end of the feeder. Some of these properties have been observed or conjectured in the literature but never mathematically proved; see Section III-C. Our simple continuous linear model allows us to prove these properties. Finally we present simulation results to demonstrate that these properties, though derived under restrictive assumptions, hold approximately also on radial networks modeled by standard discrete nonlinear DistFlow equations of [18], [19] and even when loads have different shapes.

II. Problem Formulation

A. Linear Network Model

We consider a main feeder modeled by a single line of length L consisting of a continuum of buses, each of which is indexed by its position $\xi \in [0, L]$, with the substation at position 0. The impedance per unit length of the line is given by $z(\xi) = r(\xi) + \mathrm{j}x(\xi)$, and the power injections are

This work was supported by Los Alamos National Lab through an DoE grant DE-AC52-06NA25396, DTRA through grant HDTRA 1-15-1-0003, NSF through CNS grant 1545096, EPCN grant 1619352, and CCF grant 1637598, and Skoltech through collaboration agreement 1075-MRA.

Yujie Tang is with the Electrical Engineering Department and Steven H. Low is with the Computing and Mathematical Sciences and the Electrical Engineering Departments, California Institute of Technology, Pasadena, CA 91125, USA. {ytang2, slow}@caltech.edu

denoted by $s(\xi) = p(\xi) + \mathrm{j}q(\xi)$. The continuous linearized branch-flow model is:

$$\frac{dP}{d\xi} = -p(\xi), \quad \frac{dQ}{d\xi} = -q(\xi),$$
$$\frac{dv}{d\xi} = 2(r(\xi)P(\xi) + x(\xi)Q(\xi)),$$

where $S(\xi) = P(\xi) + \mathrm{j}Q(\xi)$ denotes the power flow *towards* the substation, and $v(\xi)$ denotes the squared voltage magnitude. As discussed above this model is based on the DistFlow model of [18], [19] and builds on the ideas in [18], [19], [20], [22].

The continuous model reduces to the linear discrete model of [18], [19], [20] if we set $s(\xi) = \sum_{j=1}^{N} s_j h_\epsilon(\xi - \xi_j)$ and take the limit $\epsilon \to 0$, where s_j is the power injection of the j'th bus, ξ_j is the corresponding coordinate, and $h_\epsilon(\xi)$ tends to the Dirac delta function as $\epsilon \to 0$. Therefore we lose no modeling capability when using the continuous model.

B. Load and Storage Model

We assume that the real power injection at each location consists of two parts: one is the power consumption by the storage device $u(\xi, t)$, and the other is the sum of all other injections $\tilde{p}(\xi, t)$ which we assume to be deterministic. The background injections $\tilde{p}(\xi, t)$ can be obtained from historical data and used to solve our planning problem. We further assume that the background injection takes the form $\tilde{p}(\xi, t) = \alpha(\xi)p(t) + \beta(\xi)$ where $\alpha(\xi) > 0$. This means that all load profiles have the same shape $p(t)$, with $\alpha(\xi)$ representing the relative variation and $\beta(\xi)$ representing an offset demand.[1] This assumption is based on the observation that the electricity usage pattern of a large group of residential customers can be segmented into a relatively few set of signature load shapes [23], [24]. Without loss of generality we require the time average of $p(t)$ to be zero. Therefore the net power injection at location ξ is given by

$$p(\xi, t) = \tilde{p}(\xi, t) - u(\xi, t) = \alpha(\xi)p(t) + \beta(\xi) - u(\xi, t).$$

For the storage devices, we employ the simple model

$$\frac{\partial b(\xi, t)}{\partial t} = u(\xi, t), \quad 0 \le b(\xi, t) \le B(\xi),$$

where $b(\xi, t)$ is the energy level (SoC) at time t, and $B(\xi)$ is the energy capacity of the storage device at location ξ. This model ignores several fine features of a practical device, e.g., it ignores power limit on $u(x, t)$, round-trip inefficiency, and any effect on reactive power injections. It is however sufficient for broad structural properties of optimal placement and sizing strategy.

Load profiles often exhibit a cyclic behavior, i.e., $p(t + T) = p(t)$ for some $T > 0$. We hence consider a finite horizon $\mathbb{T} = [0, T]$ and assume that the shape satisfies $p(0) = p(T) = 0$. We require that the operation of energy storage also be cyclic, i.e., $u(\xi, 0) = u(\xi, T)$ and $b(\xi, 0) = b(\xi, T)$. The restriction on the time average of $p(t)$ then becomes

$$\int_{\mathbb{T}} p(t)\, dt = 0.$$

C. Optimal Placement and Sizing

The cost we wish to minimize is the total energy loss of the network in a cycle $\mathbb{T}$. We first use the linearized continuous model to formulate an expression for power loss. If we assume that the voltage fluctuation along the line is small compared to 1 pu, which is a good approximation in many practical scenarios, then the total power loss at time t is given by [19], [20]

$$P_{\text{loss}}(t) = \int_0^L r(\xi) \frac{P^2(\xi, t) + Q^2(\xi, t)}{v(\xi, t)}\, d\xi$$
$$\approx \int_0^L r(\xi) P^2(\xi, t)\, d\xi + \text{const},$$

where we have used the assumption that the storage devices do not consume or produce reactive power.

Although in many distribution networks the power loss is small compared to the loads, loss minimization can lead to other advantages such as increased voltage stability [25] and reduced branch power flows. This is partly why voltage and line limits are sometimes relaxed in loss minimization.

The optimal placement and sizing problem is the following:

$$\min_{\substack{b(\cdot,\cdot) \in \mathcal{B} \\ B(\cdot)}} \quad \int_{\mathbb{T}} \int_0^L r(\xi) P^2(\xi, t)\, d\xi\, dt \tag{1a}$$

$$\text{s.t.} \quad P(\xi, t) = \int_\xi^L \left(\alpha(\eta)p(t) + \beta(\eta) - \frac{\partial b(\eta, t)}{\partial t} \right) d\eta \tag{1b}$$

$$0 \le b(\xi, t) \le B(\xi), \quad \forall t \in \mathbb{T},\ \xi \in [0, L] \tag{1c}$$

$$0 \le B(\xi), \quad \forall \xi \in [0, L] \tag{1d}$$

$$\int_0^L B(\eta)\, d\eta \;=\; B_{\text{tot}} \tag{1e}$$

where $\mathcal{B}$ represents the set of all possible cyclic operations. A schedule $u^*(t) := \partial b^* / \partial t$, SoC $b^*(\xi, t)$ and storage capacity $B^*(\xi)$ are called *optimal* if they solve the optimization problem (1).

III. Optimal Solution

A. Structural Properties of Optimal Solution

We make the following assumptions on the shape $p(t)$ of the background injection $\tilde{p}(t)$, as illustrated in Figure 1, and the total storage budget B_{tot}:

- C1: $p(t)$ is continuously differentiable on $\mathbb{T}$.
- C2: $p(t)$ has only one local minimum $p_{\min}$ and one local maximum $p_{\max}$.
- C3: The total storage budget B_{tot} is not too large:

$$B_{\text{tot}} < \frac{1}{2} \int_0^L \alpha(x)\, dx \int_{\mathbb{T}} |p(t)|\, dt =: B_m$$

[1] Note that $\tilde{p}$ is background injection and it takes a negative value when it represents a load and and a positive value when it represents generation.

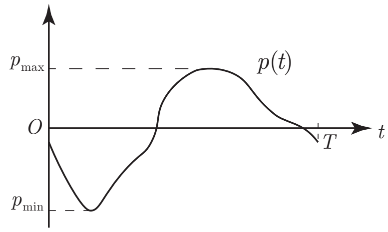

Fig. 1. An example shape $p(t)$ of background injection $\tilde{p}(t)$.

Condition C1 is not restrictive because any continuous function can be approximated by a continuously differentiable function to any given precision. Condition C2 does not hold in general. Nevertheless, the derived structural properties hold even without this assumption; see Section IV. Condition C3 is assumed since it can be shown that when $B_{\text{tot}} \geq B_m$, adding more storage will not improve the objective any more.

Theorem 1 (Structural properties): Suppose the shape $p(t)$ satisfies conditions C1, C2 and the storage budget B_{tot} condition C3. Then there exists a location $\xi^* \in (0, L]$, and for each location $\xi \in [0, L]$ there are two thresholds $\phi_+(\xi)$ and $\phi_-(\xi)$ such that the optimal schedule $u^*(\xi, t)$ and the optimal capacity $B^*(\xi)$ satisfy the following properties.

1) Optimal storage capacity $B^*(\xi) = 0$ at every location $\xi < \xi^*$. At each location $\xi \geq \xi^*$, the scaled optimal storage capacity increases as one moves away from the substation, i.e., $B^*(\xi)/\alpha(\xi) > 0$ is an increasing function of ξ on $[\xi^*, L]$.
2) At each location $\xi \in [\xi^*, L]$, the storage device charges when the shape of the background injection exceeds the high threshold and discharges when it drops below the low threshold, i.e., $u^*(\xi, t) \geq 0$ when $p(t) > \phi_+(\xi)$, $u^*(\xi, t) \leq 0$ when $p(t) < \phi_-(\xi)$, and $u^*(\xi, t) = 0$ otherwise.
3) The larger the storage budget B_{tot}, the closer ξ^* is to the substation, i.e., there is a continuous bijection between $B_{\text{tot}} \in [0, B_m)$ and the corresponding $\xi^* \in (0, L]$, and ξ^* decreases as B_{tot} increases.
4) The larger the storage budget B_{tot}, the higher the storage capacity $B^*(\xi) > 0$ for $\xi > \xi^*$.
5) The high threshold function $\phi_+ : [0, L] \to [0, +\infty)$ is a decreasing function with $\phi_+(\xi^*) = p_{\max}$, and the low threshold function $\phi_- : [0, L] \to (-\infty, 0]$ is an increasing function with $\phi_-(\xi^*) = p_{\min}$.

Define the time intervals where $p(t)$ exceeds the high threshold $\phi_+(\xi)$ or drops below the low threshold $\phi_-(\xi)$:

$$\begin{aligned} \mathbb{T}_+(\xi) &= \{t \in \mathbb{T} : p(t) > \phi_+(\xi)\} \\ \mathbb{T}_-(\xi) &= \{t \in \mathbb{T} : p(t) < \phi_-(\xi)\} \end{aligned} \tag{2}$$

Figure 2a shows how to obtain the sets $\mathbb{T}_\pm(\xi)$ from $\phi_\pm(\xi)$ and $p(t)$.

Indeed the optimal schedule $u^*(\xi, t)$, the optimal storage capacities $B^*(\xi)$, and the SoC trajectories $b^*(\xi, t)$ can be explicitly solved.

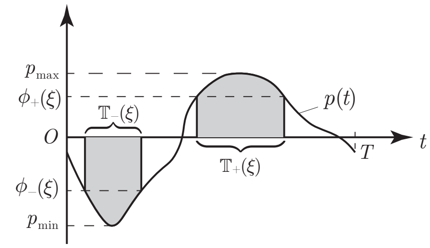

(a) Determining $\mathbb{T}_+(\xi)$ and $\mathbb{T}_-(\xi)$.

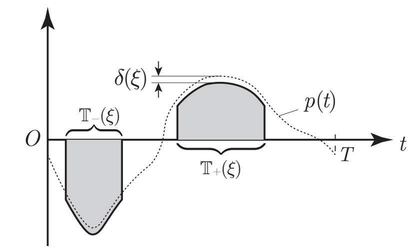

(b) Adding offset $\delta(\xi)$. This offset ensures that $\int_{\mathbb{T}}(p(t) - \delta(\xi))\, dt = 0$ and $b(\xi, 0) = b(\xi, T)$.

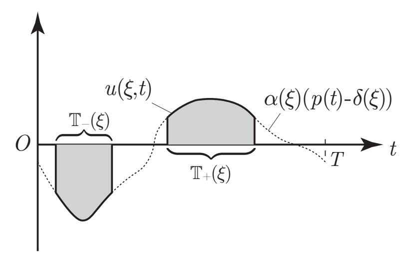

(c) Scaling by $\alpha(\xi)$.

Fig. 2. Illustration of $u^*(\xi, t)$ at an $\xi > \xi^*$ given by (2), (3) and (4).

Theorem 2 (Optimal solution): Suppose the shape $p(t)$ satisfies conditions C1, C2 and the storage budget B_{tot} condition C3. Then the optimal schedule $u^*(\xi, t)$, SoC trajectory $b^*(\xi, t)$ and storage capacity $B^*(\xi)$ are given by:

$$\begin{aligned} u^*(\xi, t) &= \begin{cases} \alpha(\xi)(p(t) - \delta(\xi)), & t \in \mathbb{T}_+(\xi) \cup \mathbb{T}_-(\xi) \\ 0, & \text{otherwise} \end{cases} \\ b^*(\xi, t) &= \int_{\inf \mathbb{T}_+(\xi)}^{t} u^*(\xi, t)\, dt \\ B^*(\xi) &= \int_{\mathbb{T}_+(\xi)} u^*(\xi, t)\, dt \end{aligned} \tag{3}$$

where

$$\delta(\xi) := \frac{\int_{\mathbb{T}_+(\xi) \cup \mathbb{T}_-(\xi)} p(t)\, dt}{\int_{\mathbb{T}_+(\xi) \cup \mathbb{T}_-(\xi)} dt} \quad \text{for } \xi > \xi^* \tag{4}$$

Figure 2b and 2c show the steps of calculating the optimal schedule $u^*(\xi, t)$.

We now discuss the implications of these results.

B. Optimal Storage Placement and Capacity

Theorem 1(5) implies that, for all $\xi < \xi^*$, $\phi_+(\xi) > p_{\max} \geq p(t)$ and $\phi_-(\xi) < p_{\min} \leq p(t)$, so $\mathbb{T}_+(\xi) = \mathbb{T}_-(\xi) = \varnothing$. This implies that $B^*(\xi) = 0$ for $\xi < \xi^*$, i.e., no storage device is placed before the location ξ^*, as stated in Theorem 1(1).

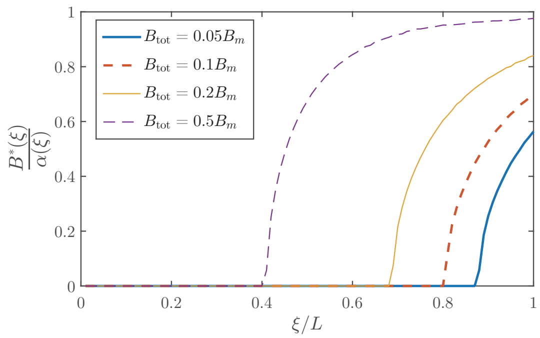

Fig. 3. Example curves of $B^*(\xi)/\alpha(\xi)$. The unit of the y axis is $\left(\int_0^L \alpha(\xi)\, d\xi\right)^{-1} B_m = \frac{1}{2}\int_{\mathbb{T}} |p(t)|\, dt$.

For $\xi > \xi^*$, C2 implies that $\mathbb{T}_+(\xi)$ is a nontrivial interval. Theorem 2 then implies that $B^*(\xi) > 0$, i.e., energy storage will be deployed at all locations $\xi > \xi^*$. Hence ξ^* divides the feeder into two contiguous segments: storage is not deployed in the segment containing the substation but everywhere in the other segment.

Theorem 1(3) and (4) show that if we have a higher storage budget B_{tot} then the storage capacity $B^*(\xi)$ at *every* location $\xi > \xi^*$ should increase. Moreover the continuous decreasing *bijection* between $B_{\text{tot}} \in [0, B_m)$ and $\xi^* \in (0, L]$ implies that, when the budget B_{tot} is small, storage will be deployed only near the end of the line, and as we increase the budget, ξ^* moves towards the substation and the segment with storage enlarges. As $B_{\text{tot}} \to B_m$, $\xi^* \to 0$ and storage will be deployed on the whole line.

Now fix the budget B_{tot} and consider how $B(\xi)$ varies with ξ. According to Theorem 2

$$B^*(\xi) = \alpha(\xi) \int_{\mathbb{T}_+(\xi)} (p(t) - \delta(\xi))\, dt$$

This equation suggests that roughly a larger $\alpha(\xi)$ yields a larger $B^*(\xi)$, which is in accordance with our intuition that a larger power fluctuation requires a larger storage device to flatten the power injection.

The monotonicity of $B^*(\xi)/\alpha(\xi)$ in Theorem 1(1) is an important property that has not been studied before. To illustrate its implication, consider the special case that $\alpha(\xi)$ is uniform. Then Theorem 1(1) implies that more storage capacity should be placed as we move from the substation towards the end of the line. This is partly due to the fact that power injections near the end of the line have a greater effect on the power flow on the whole distribution line than power injections near the substation. Figure 3 shows some examples of $B^*(\xi)/\alpha(\xi)$ as a function of ξ, using the shape curve in Figure 1.

These structural properties of $B^*(\xi)$ and $B^*(\xi)/\alpha(\xi)$ hold for discrete networks as well. Specifically, let $\mathcal{N} = \{0, \ldots, N\}$ be the set of buses in a discrete linear network, where Bus 0 is the substation and the parent of bus i is Bus $i-1$. Let the power injection at bus i be

$$\tilde{p}_i(t) = \alpha_i p(t) + \beta_i. \tag{5}$$

Then we can prove the following properties of the optimal solution for discrete linear network.

Theorem 3 (Discrete linear network): 1) There exists $i^* \in \mathcal{N}\backslash\{0\}$ such that $B_i^* = 0$ for $i < i^*$ and $B_i^* > 0$ for $i \geq i^*$. When B_{tot} is small enough, $i^* = N$, and i^* moves towards the substation as B_{tot} increases.
2) For a fixed i, B_i^* increases as B_{tot} increases.
3) For a fixed B_{tot}, B_i^*/α_i increases as i increases [2].

If $B_{\text{tot}} \geq B_m$, it can be shown that we have enough energy capacity to make the power injections totally flat at every location, which is not an interesting case for our study.

C. Optimal Schedule

The optimal schedule $u^*(\xi, t)$ (3) in Theorem 2 is a load shifting policy that shaves the peak and fills the valley. Specifically, for each fixed $\xi > \xi^*$, since $\mathbb{T}_+(\xi)$ and $\mathbb{T}_-(\xi)$ are time intervals that respectively enclose the maximum and minimum background injection shape $p(t)$, (3) means that, around the peak and the valley of $p(t)$, the optimal schedule follows the background power injection $\tilde{p}(\xi, t)$ with an offset; Outside the region around the peak or the valley of $p(t)$, u^* keeps the SoC unchanged. The monotonicity of $\phi_+(\xi)$ and $\phi_-(\xi)$ implies that $\mathbb{T}_+(\xi)$ and $\mathbb{T}_-(\xi)$ expands as ξ increases. This means that the amount of time for charging and discharging increases as we move towards the end of the line. Load shifting policies have been studied with a single storage device in [26], [27], [28], but have not be shown to be optimal with multiple storage devices on a power network.

IV. Simulations and Discussion

We now present simulation results which show that the structural properties of Section III approximately hold even when some of the restrictive assumptions are relaxed. In particular all our simulations use the original nonlinear DistFlow model of [18], [19] instead of the continuous linear model we used to analytically derive these properties. To find an optimal solution we use the second-order cone relaxation developed in [29], [30], [31]. All relaxations have been checked to be exact.

A. Linear Networks

The linear network for simulation is a subnetwork of the IEEE 34-bus feeder. We use the path connecting bus 848 and the substation as our linear network (see Figure 4), adopt its line impedances and shunt capacitors, and simplify it as a single-phase network with all constant power loads. The peak loads of the buses are given in Table I, which are adapted from the original test feeder data. The voltage regulator taps are set and fixed so that the voltage magnitude of each bus is within $[0.95, 1.05]$.

We first relax assumption C2. Figure 5 shows the averaged domestic load profile in Jan. 2015 from Southern California Edison [32], which has two peaks and two valleys. Assuming that all load profiles have this shape and assume that the load

[2] If $\alpha_i = 0$, then we have $B_i^* = 0$ and the quantity B_i^*/α_i will be undefined, but after we eliminate these buses, B_i^*/α_i is still an increasing function of i.

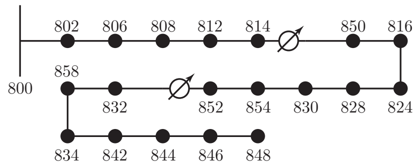

Fig. 4. The linear network for simulation, adapted from IEEE 34-bus feeder.

TABLE I
PEAK LOADS OF THE LINEAR NETWORK

Bus No.	800	802	806	808	812
Peak kW	0	0	55	16	0
Peak kVAr	0	0	29	8	0
Bus No.	814	850	816	824	828
Peak kW	0	0	169	45	4
Peak kVAr	0	0	87	22	2
Bus No.	830	854	852	832	858
Peak kW	52	4	0	450	17
Peak kVAr	23	2	0	225	8
Bus No.	834	842	844	846	848
Peak kW	415	0	414	45	83
Peak kVAr	236	0	320	23	59

at bus i equals this profile multiplied by a scaling factor α_i. We compute the optimal schedule u^* and optimal storage placement B^*. Figure 6 shows the optimal B_i^* for different B_{tot}. In all the cases, there exists a bus i^* separating the segments with and without storage. Furthermore, the function B_i^*/α_i is increasing in i for each B_{tot} value. For bus 848, when B_{tot} increases from $450\,\text{kWh}$ to $600\,\text{kWh}$, the corresponding B_i^* is reduced by a small amount, contradicting Theorem 1(4). This is a consequence of the nonlinearity of the power flow equations. We have also run other test cases and have found that this kind of violation does not occur very often.

Next we relax the assumption that all loads have the same shape $p(t)$. Our simulations show that the structural properties generally do not hold if load shapes are significantly different at different buses. Here we consider the situations where this assumption holds approximately: suppose the background injection is given by

$$\tilde{p}_i(t) = \alpha_i(p(t) + \delta p_i(t)) + \beta_i,$$

where $\delta p_i(t)$ represents the deviation from the assumption of uniform shape. We assume that for a fixed i, $\delta p_i(t)$

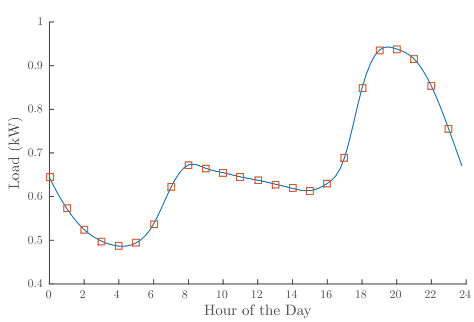

Fig. 5. Load profile with two peaks and two valleys.

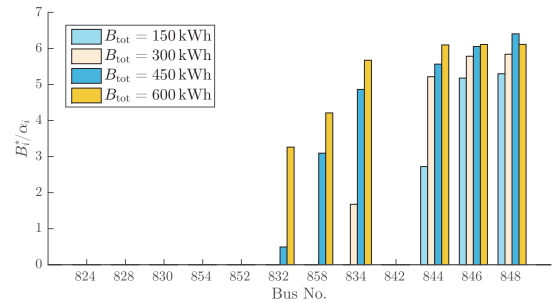

Fig. 6. Optimal B_i^*/α_i when the load shape is given by Figure 5. Since there is no power injection at bus 842, the corresponding quantity B_i^*/α_i is ignored. No storage is deployed at any bus before 824.

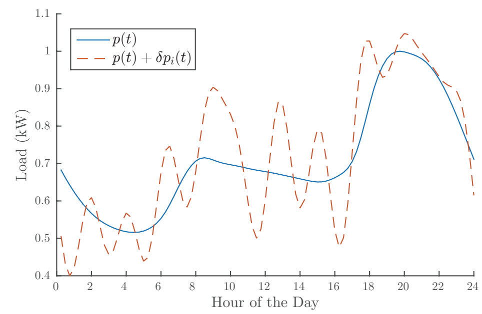

Fig. 7. Deviation pattern of the load shape.

is generated from a Gaussian white noise with bandwidth $1/2$ hour^{-1}, and at different locations, the stochastic processes $(\delta p_i(t) : t \in \mathbb{T})$ are independent of each other. The magnitude of this deviation is given by

$$\frac{\max_{t\in\mathbb{T}} |\delta p_i(t)|}{\max_{t\in\mathbb{T}} p(t) - \min_{t\in\mathbb{T}} p(t)} = 0.5.$$

Figure 7 shows an example pattern.

Figure 8 shows a set of typical results for different storage budgets B_{tot}. The distribution line can still roughly be segmented into two parts, one with storage and one without storage. Even though B_i^*/α_i is no longer strictly monotonic in i, monotonicity is still a reasonable approximation. Further simulations suggest that these structural properties are robust against perturbations as long as $\max_{t\in\mathbb{T}} |\delta p_i(t)|$ are small and B_{tot} is small.

B. Radial Networks

We now study these structural properties on a radial network. We use a simplified version of the IEEE 123-bus test feeder [33] for our simulations. We employ its network topology, line impedances, shunt capacitors and default switch settings, regard the loads as the peak loads, and simplify it as a single-phase network with all constant power loads. We use the load shape in Figure 5, and assume that the load at bus i equals this profile multiplied by a scaling factor α_i.

The results are shown in Figure 9. We use solid dots to represent buses with nonzero injections and hollow circles for buses with zero injections. The optimal storage placement B_i^* is represented by differently colored solid circles for different

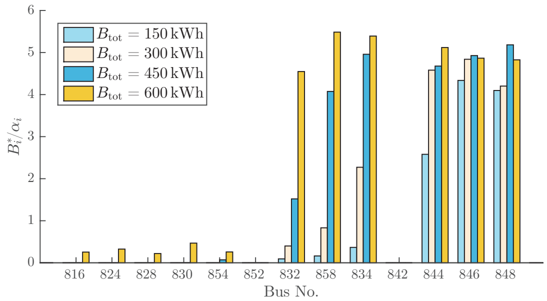

Fig. 8. Optimal B_i^*/α_i when the load profiles deviate from the ideal case. Since there are no power injections at Bus 842 and 852, the corresponding B_i^*/α_i are undefined. All buses before 816 have no storage allocated.

$B_{\rm tot}$. For bus i with nonzero power injections, the radius of a colored circle is proportional to B_i^*/α_i. We make the following observations:

1) B_i^* increases for each i as $B_{\rm tot}$ increases.
2) Let k be a leaf node and let ℓ_k be the unique path connecting k and the substation. Then apart from nodes where B_i^*/α_i is undefined, B_i^*/α_i is monotonically increasing along path ℓ_k as we move from the substation to the leaf k.
3) Storage devices are distributed typically far from the substation.

These properties are consistent with Theorem 1 for linear networks under restrictive assumptions. Simulation also shows that, for a bus with no power injections, the corresponding B_i^* is zero. These observations suggest that, the structural results we derived for linear networks also hold for general radial networks.

C. Robustness to Load Profile

The optimal power flow (OPF) approach to storage placement and sizing problem used in this (as well as many other) papers relies on a forecast load profile $\tilde{p}(t)$. The solution jointly optimizes the storage capacity B^* and charging/discharging schedule u^*. Once storage B^* is deployed, however, optimal schedule u^* will need to be determined with respect to actual load profiles, with fixed storage capacities. How robust is the optimal placement and sizing B^* to errors in load forecast and hence charging/discharging schedule?

We have conducted some preliminary simulations regarding this problem. We first assume that all loads have the same shape shown in Figure 5, and compute the optimal storage placement B_i^0 and the loss reduction. Then we fix the storage placement to be B_i^0, perturb the background power injections $\tilde{p}(t)$, and compute the corresponding loss reduction by optimizing *only* over charging/discharging schedule $u_i(t)$. This simulates storage in operation. Using the perturbed $\tilde{p}(t)$, we solve again the joint optimization of storage capacities B_i^* and schedule u_i^*. This is unrealistic because storage placement and sizing cannot be changed in operation when load profiles change, but serves as a benchmark. The results are shown in the middle and right column of Table II. The simulation network is that shown in Figure 4 and $B_{\rm tot} = 600\,\rm kWh$. We perturb the power injections the same way as in Section IV-A. The difference in performance is negligible and suggests that the OPF approach to storage placement and sizing is robust.

TABLE II

LOSS REDUCTION WITH PERTURBED PROFILES

	Loss reduction with B_i^0	Optimal loss reduction
No perturbation	48.78 kWh	
Perturbed Inst. 1	46.72 kWh	46.77 kWh
Perturbed Inst. 2	51.38 kWh	51.39 kWh
Perturbed Inst. 3	47.65 kWh	47.66 kWh

V. CONCLUSION

In this paper, we have studied the problem of optimal placement and sizing of energy storage in distribution networks. We consider a linear network modeling a main feeder and formulate the problem as an optimal power flow problem using a linearized continuous power flow model. We derive explicitly the optimal solution when all loads have the same shape and that the shape has only one peak and one valley, and prove several monotonicity properties of the optimal solution. We have presented simulations results that demonstrate that these structural properties hold approximately for general radial networks modeled by the standard discrete nonlinear power flow model even when loads have different shapes.

There are several directions for future research. First, a theory for general radial networks will be a natural topic for future study, and we have got some interesting results on this which will appear in a future paper. Second, a theory with less load profile assumptions and better power flow models will also be of great interest. For example, it will be useful to quantitatively describe the effect of deviations of load profiles from the common load shape; adding line limits to the model will also be interesting. Third, the present theory is based on a deterministic program, where load profiles are obtained from historical data with no uncertainties. Although the discussion in Section IV.C suggests that our theory is still applicable when uncertainties are small, it will be interesting to model uncertainties directly and see the consequences.

REFERENCES

[1] J. P. Barton and D. G. Infield, "Energy storage and its use with intermittent renewable energy," *IEEE Trans. Energy Conversion*, vol. 19, no. 2, pp. 441–448, June 2004.

[2] J. V. Paatero and P. D. Lund, "Effect of energy storage on variations in wind power," *Wind Energy*, vol. 8, no. 4, pp. 421–441, 2005.

[3] S. C. Smith, P. K. Sen, and B. Kroposki, "Advancement of energy storage devices and applications in electrical power system," in *Proc. IEEE Power and Energy Soc. General Meeting*, 2008, pp. 1–8.

[4] T. Kousksou, P. Bruel, A. Jamil, T. El Rhafiki, and Y. Zeraouli, "Energy storage: Applications and challenges," *Solar Energy Materials and Solar Cells*, vol. 120, pp. 59–80, 2014.

[5] A. Faghih, M. Roozbehani, and M. A. Dahleh, "On the value and price-responsiveness of ramp-constrained storage," *Energy Conversion and Management*, vol. 76, pp. 472–482, 2013.

[6] Y. Xu and L. Tong, "On the operation and value of storage in consumer demand response," in *Proc. 53rd IEEE Conf. Decision and Control (CDC)*, 2014, pp. 205–210.

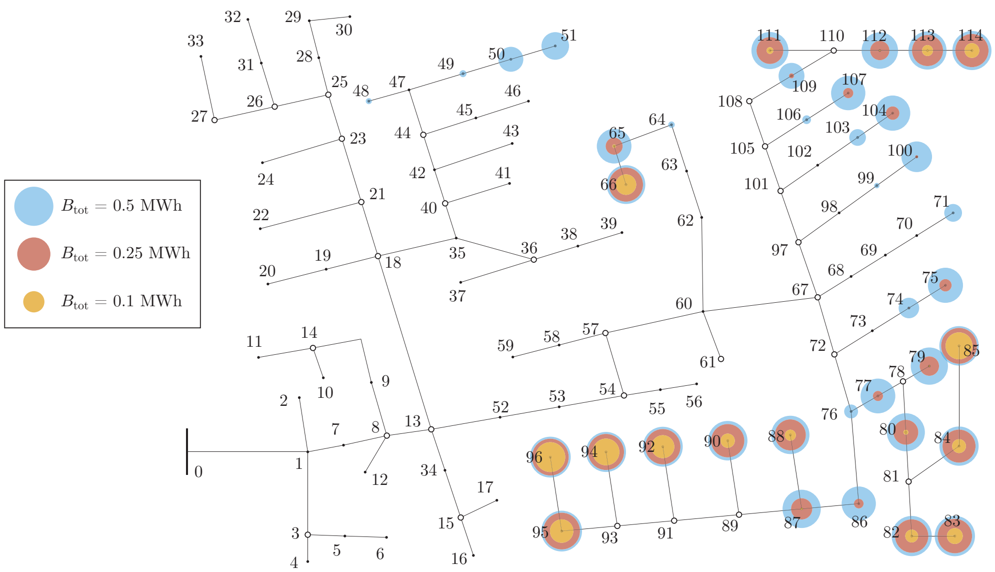

Fig. 9. Optimal storage placement for the simplified IEEE 123-bus test feeder. Solid dots represent buses with power injections, and hollow circles represent buses with no power injections. The radius of each colored solid circle is proportional to B_i^*/α_i, and different colors correspond to different B_{tot}.

[7] P. Harsha and M. Dahleh, "Optimal management and sizing of energy storage under dynamic pricing for the efficient integration of renewable energy," *IEEE Trans. Power Systems*, vol. 30, no. 3, pp. 1164–1181, May 2015.

[8] S. Bose, D. F. Gayme, U. Topcu, and K. M. Chandy, "Optimal placement of energy storage in the grid," in *Proc. 51st IEEE Conf. Decision and Control (CDC)*, 2012, pp. 5605–5612.

[9] A. Castillo, X. Jiang, and D. F. Gayme, "Lossy DCOPF for optimizing congested grids with renewable energy and storage," in *Proc. American Control Conf.*, 2014, pp. 4342–4347.

[10] D. Gayme and U. Topcu, "Optimal power flow with large-scale storage integration," *IEEE Trans. Power Systems*, vol. 28, no. 2, pp. 709–717, May 2013.

[11] C. Thrampoulidis, S. Bose, and B. Hassibi, "Optimal placement of distributed energy storage in power networks," *IEEE Trans. Automatic Control*, 2015.

[12] Y. Kanoria, A. Montanari, D. Tse, and B. Zhang, "Distributed storage for intermittent energy sources: Control design and performance limits," in *Proc. 49th Allerton Conf. Communication, Control, and Computing*, 2011, pp. 1310–1317.

[13] J. Qin, Y. Chow, J. Yang, and R. Rajagopal, "Distributed online modified greedy algorithm for networked storage operation under uncertainty," *IEEE Trans. Smart Grid*, 2015.

[14] Y. M. Atwa and E. F. El-Saadany, "Optimal allocation of ESS in distribution systems with a high penetration of wind energy," *IEEE Trans. Power Systems*, vol. 25, no. 4, pp. 1815–1822, Nov. 2010.

[15] H. Pandzic, Y. Wang, T. Qiu, Y. Dvorkin, and D. S. Kirschen, "Near-optimal method for siting and sizing of distributed storage in a transmission network," *IEEE Trans. Power Systems*, vol. 30, no. 5, pp. 2288–2300, Sept. 2015.

[16] K. Dvijotham, S. Backhaus, and M. Chertkov, "Operations-based planning for placement and sizing of energy storage in a grid with a high penetration of renewables," 2011, arxiv preprint arXiv:1107.1382.

[17] S. Bose and E. Bitar, "The locational marginal value of energy storage," preprint.

[18] M. E. Baran and F. F. Wu, "Optimal sizing of capacitors placed on a radial distribution system," *IEEE Trans. Power Delivery*, vol. 4, no. 1, pp. 735–743, Jan. 1989.

[19] ——, "Network reconfiguration in distribution systems for loss reduction and load balancing," *IEEE Trans. Power Delivery*, vol. 4, no. 2, pp. 1401–1407, Apr. 1989.

[20] J. A. Taylor and F. S. Hover, "Convex models of distribution system reconfiguration," *IEEE Trans. Power Systems*, vol. 27, no. 3, pp. 1407–1413, Aug. 2012.

[21] S. H. Low, "Convex relaxation of optimal power flow, I: Formulations and equivalence," *IEEE Trans. Control of Network Systems*, vol. 1, no. 1, pp. 15–27, March 2014.

[22] D. Wang, K. Turitsyn, and M. Chertkov, "Distflow ODE: Modeling, analyzing and controlling long distribution feeder," in *Proc. 51st IEEE Conf. Decision and Control (CDC)*, 2012, pp. 5613–5618.

[23] B. A. Smith, J. Wong, and R. Rajagopal, "A simple way to use interval data to segment residential customers for energy efficiency and demand response program targeting," in *ACEEE Summer Study on Energy Efficiency in Buildings*, 2012.

[24] J. Kwac, J. Flora, and R. Rajagopal, "Household energy consumption segmentation using hourly data," *IEEE Trans. Smart Grid*, vol. 5, no. 1, pp. 420–430, Jan. 2014.

[25] M. A. Kashem and M. Moghavvemi, "Maximizing radial voltage stability and load balancing via loss minimization in distribution networks," in *Proc. Int. Conf. Energy Management and Power Delivery*, vol. 1, 1998, pp. 91–96.

[26] M. Chandy, S. Low, U. Topcu, and H. Xu, "A simple optimal power flow model with energy storage," in *Proc. 49th IEEE Conf. Decision and Control (CDC)*, 2010, pp. 1051–1057.

[27] I. Koutsopoulos, V. Hatzi, and L. Tassiulas, "Optimal energy storage control policies for the smart power grid," in *Proc. IEEE Int. Conf. Smart Grid Commun.*, 2011, pp. 475–480.

[28] G. Bao, C. Lu, Z. Yuan, and Z. Lu, "Battery energy storage system load shifting control based on real time load forecast and dynamic programming," in *Proc. 8th IEEE Int. Conf. Automation Science and Engineering*, 2012, pp. 815–820.

[29] M. Farivar, C. R. Clarke, S. H. Low, and K. M. Chandy, "Inverter var control for distribution systems with renewables," in *Proc. IEEE Int. Conf. Smart Grid Commun.*, 2011, pp. 457–462.

[30] M. Farivar and S. H. Low, "Branch flow model: Relaxations and convexification (parts I, II)," *IEEE Trans. Power Systems*, vol. 28, no. 3, pp. 2554–2572, Aug. 2013.

[31] L. Gan, N. Li, U. Topcu, and S. H. Low, "Exact convex relaxation of optimal power flow in radial networks," *IEEE Trans. Automatic Control*, vol. 60, no. 1, pp. 72–87, Jan. 2015.

[32] [Online]. Available: https://www.sce.com/wps/portal/home/regulatory/load-profiles

[33] W. H. Kersting, "Radial distribution test feeders," in *Proc. IEEE Power Engineering Soc. Winter Meeting*, vol. 2, 2001, pp. 908–912.